2017-08-04

High-resolution IKONOS satellite imagery for normalized difference vegetative index-related assessment applied to land clearance studies

Lavers, CR

10.1117/1.JRS.11.035008
Journal of Applied Remote Sensing
SPIE-Intl Soc Optical Eng

High-resolution IKONOS satellite imagery for normalized difference vegetative index-related assessment applied to land clearance studies

Chris R. Lavers[a,*] **and Travis Mason**[b]
[a]Plymouth University, Britannia Royal Naval College, Marine School of Engineering, Dartmouth, Devon, United Kingdom
[b]National Oceanography Centre, Southampton Channel Coastal Observatory, European Way, Southampton, United Kingdom

Abstract. High-resolution satellite imagery permits verification of human rights land clearance violations across international borders as a result of unstable regimes or socio-economic upheaval. Without direct access to these areas to validate allegations of human rights abuse, the use of remote sensing tools, techniques, and data is extremely important. Humanitarian assessment can benefit from software-based solutions, involving radiometrically calibrated normalized difference vegetation index and temporal change imagery. We discuss the introduction of a matrix filter approach for change detection studies to help assist rapid building detection over large search areas against a bright background to evaluate internally displaced people in the 2005 Porta Farm Zimbabwe clearances. Future wide-scale near real-time space-based monitoring with a range of digital filters would be of great benefit to international human rights observers and human rights networks. © *2017 Society of Photo-Optical Instrumentation Engineers (SPIE)* [DOI: 10.1117/1.JRS.11.XX.XXXXXX]

Keywords: land clearance; high-resolution normalized difference vegetation index and temporal changes; high-pass filter; man-made disaster.

Paper 170018L received Jan. 19, 2017; accepted for publication Jul. 10, 2017.

1 Introduction and Historical Background

Satellite-based imagery now provides an essential geographical tool to help remotely confirm allegations of human rights abuse, especially large-scale land clearing. Resource, political, or ethnic-driven conflicts place human assessors in danger, notably if a party does not want operations seen, potentially by global media. As nongovernmental workers are "barred" on the pretext of safety from conflict areas, satellite imagery may be the only recourse to analyze and study these incidences.

Large-scale land clearance can be a consequence of unstable economies or regimes, increased economic globalization or climate change. These changes may exacerbate national instabilities affecting those at the bottom of the socio-economic scale hardest.[1] Frequent conflict, economic hardship, or population displacement will occur under such pressure, so documenting such cases may help provide baseline data to mitigate similar future events. From 2005 to 2006, confirmed violations occurred across Zimbabwe, clearing well-established communities, such as the small-scale farming and husbandry of Porta Farm. In May 2005, the government began Operation Restore Order (or Murambatsvina, "clear the dirt," in the Shona language), a series of forced evictions, demolishing homes and businesses. One report estimated the total Zimbabwe internally displaced people number in this period at 700,000.[2] In late June 2005, the government conducted the clearance after a long legal fight.[3] In July 2005, bulldozers executed the main demolition phase with the United Nations human rights monitors reporting several deaths,

*Address all correspondence to: Chris R. Lavers, E-mail: christopher.lavers@plymouth.ac.uk

1931-3195/2017/$25.00 © 2017 SPIE

including children. Under international law, forced evictions or demolition of deemed illegal structures is itself illegal. The United Nations Commission for Human Rights states "the practice of forced evictions constitutes a gross violation of human rights, in particular the right to adequate housing."[4] The societal implications and a critical overview of the background planning-related issues and future implications surrounding Porta Farm are discussed elsewhere.[5]

We have previously used image processing methods to observe several regions of international human rights concern in Sudan,[6] Burma,[6] and Zimbabwe.[7] We quantified them and reviewed the challenges in confirming eyewitness allegations, vital for effective response. We focus, here, on quantifying land clearance impact at the Porta Farm land clearance in 2005, one of many recorded displacements in the 2005 to 2006 clearances affecting townships across Zimbabwe. High-resolution human rights satellite monitoring was proposed in 1999,[8] but it was not until sensors with 1-m or less resolution (e.g., such as IKONOS 2 and Quickbird 2) made it feasible for commercial surveillance applications. Satellite imagery provides key tools for detailed map making vital for distribution of key resources, such as food and water, (e.g., United Nations Institute for Training and Research satellite imagery products). We focus, here, on quantified man-made population displacement-derived image products with or without full radiometric calibration, applicable to mass burial detection[9] and other conflict-driven factors.[10] Our main aim was to evaluate if IKONOS could accurately image a reported clearance, quantify it, or outline existing buildings. Substantial work on mapping destroyed building structures has been conducted by the American Association for the Advancement of Science;[11] however, none of its work has looked at multispectral changes due to man-made building removal with consequent land cover changes. This study's originality uses both a multispectral approach and the use of a high-pass filter.

2 Methodology

2.1 *Study Area*

A map of the study area of Porta Farm is shown in Fig. 1 with the study area indicated with reference to Harare the capital of Zimbabwe. It was important to obtain imagery both before and after the alleged land clearance covering Porta Farm.

2.2 *Satellite Data and Image Extraction*

The IKONOS 2 land clearance imagery covers the Porta Farm study area having rectangular coordinates approximately: northwest latitude $= -17.84°$, northwest longitude $= 30.75°$,

Fig. 1 Overview of study area showing Porta Farm in Zimbabwe © C. Lavers (2017).

southeast latitude = −17.88°, and southeast longitude = 30.80°, taken on two dates: July 25, 2000, and September 15, 2006. High-resolution satellite data from the IKONOS satellite were acquired over Porta Farm, Zimbabwe, in three visible 4-m multispectral bands with 1-m panchromatic data on June 25, 2000, and September 15, 2006. The multispectral data were used to obtain the radiometrically calibrated normalized difference vegetative index (NDVI). We selected red and near-infrared (NIR) 4-m bands of the Porta Farm region for the NDVI assessment, while panchromatic data were used to help filtering operations.

ArcGIS 10 (version 10.2 released on July 30, 2013) under license from ESRI (Redlands, California) was used to open large GeoTiff source files and to map buildings located in imagery taken before the land clearance. ArcGIS 10 extracted overlapped regions of imagery in different spectral bands for the relevant different dates and to create a map of buildings removed. Located buildings of interest were recorded by digitizing polygons using ArcGIS 10.

2.3 *Image Data Processing*

The necessary methodology, as shown in Fig. 2, would thus take the digital number (DN) values recorded by the sensor, convert the DN values to at-sensor spectral radiance, then convert the spectral radiance to at-sensor apparent reflectance, followed by the removal of atmospheric effects due to scattering and absorption (the atmospheric correction) to yield the reflectance of pixels at the earth's surface. IKONOS imagery from the GeoEye Foundation archive was provided geometrically rectified for both dates. An appropriate radiometric calibration was then applied to convert the DN values to at-sensor spectral radiance and then to convert the spectral radiance to at-sensor apparent reflectance.[12] This correction was followed by the removal of atmospheric effects due to absorption and scattering with the second simulation of a satellite signal in the Solar Spectrum-Vector (6SV) method used,[13,14] yielding the reflectance of pixels at the earth's surface. The 6S code enables accurate simulations of satellite observations, accounting for elevated targets, use of anisotropic and Lambertian surfaces, and calculation of gaseous absorption. The code is based on the method of successive orders of scattering approximations.

2.4 *Land Use/Cover Change Detection and Analysis*

2.4.1 *Multispectral approach*

Landsat Thematic Mapper is a multispectral satellite providing visible and NIR imagery, routinely used to characterize urban areas, monitor land cover and land use, or manage change. IKONOS 2 is also a multispectral satellite but with 1-m panchromatic resolution and four 4-m bands (blue 0.42 to 0.52, green 0.52 to 0.60, red 0.63 to 0.69, and NIR 0.76 to 0.90 μm respectively). IKONOS panchromatic and 4-m band combinations provide images similar to Landsat Thematic Mapper products. As stated, our primary aim was to evaluate if IKONOS could accurately image a clearance and quantify it. Although sometimes buildings are removed in stages, or involve construction, e.g., huts for military personnel or building workers, the Porta Farm clearance was accomplished in one act. Manual identification of removed building structures was time-consuming, and it is more efficient to identify large-scale clearance with minimal human input. To aid our objective, a predetection nonradiometric MATLAB® process was chosen to locate large change areas quickly for human rights and media-related analysis similar to the Landsat NDVI. Landsat NDVI-derived products provide several indices related to leaf area, biomass, or physiological function.[15] Our present humanitarian NDVI-related outputs do not require IKONOS radiometric calibration,[12] which is based on Landsat methodology.[16] Comparative analysis of IKONOS, Spot, and Enhanced Thematic Mapper Plus data considers different spectral band sensitivities,[17] but IKONOS radiometrically calibrated NDVI is not identical to Landsat NDVI, due to selected spectral band differences, and with IKONOS there are less band comparisons available. Human rights observers are not primarily interested in radiometric image products, so nonradiometric assessment is legitimate. However, NDVI-related work, as an impact assessment factor on internally displaced people communities, might be necessary in certain cases. Images, therefore, require geometric correction and coregistration for images taken

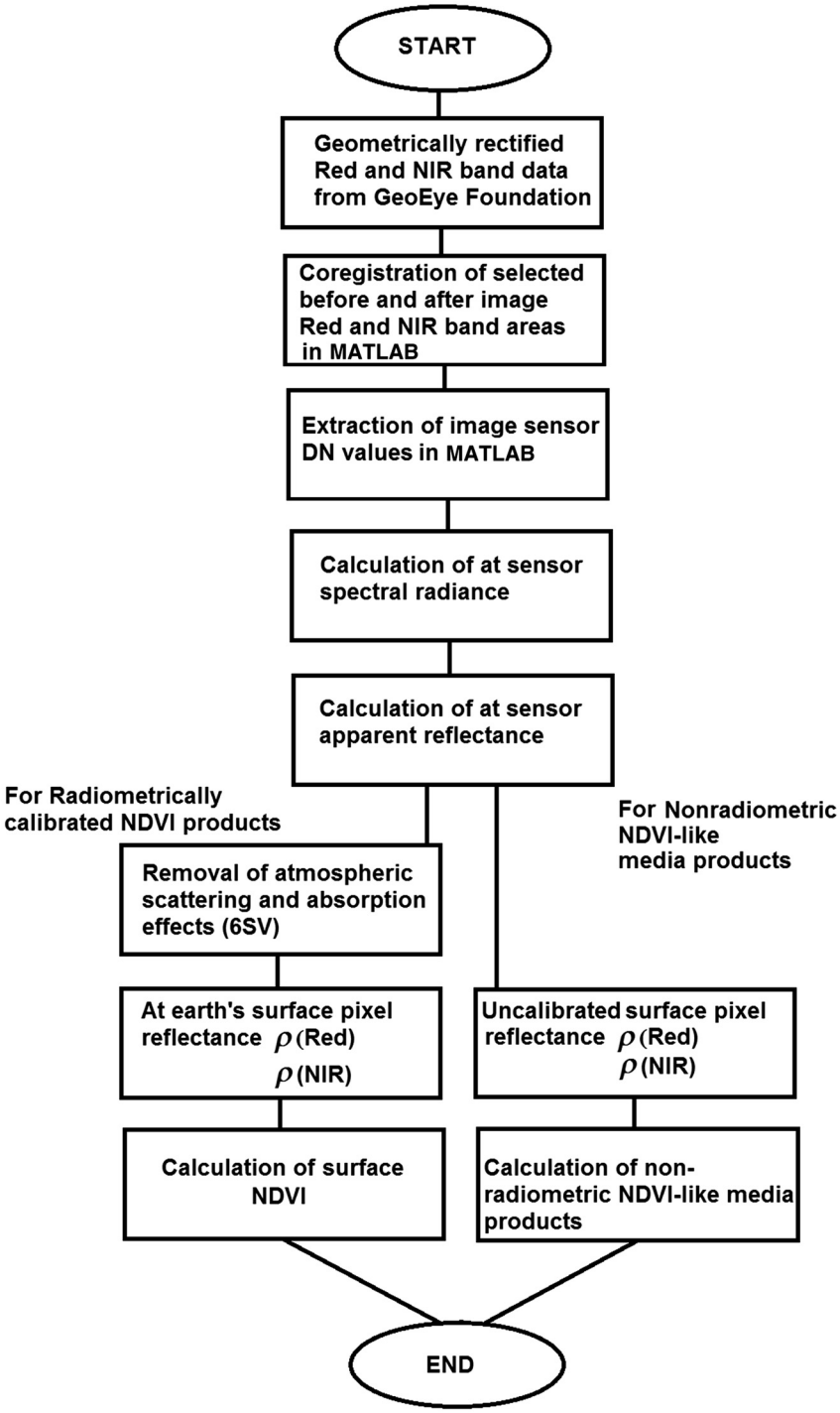

Fig. 2 Methodology of workflow analysis.

on different dates, with additional calibration to provide at-aperture spectral radiance and at-surface reflectance to correctly calculate vegetation products (see Sec. 3.3).

For large-area assessment in the analysis, we used MATLAB® software (version 2013b released on September 6, 2013, The MathWorks Inc., Natick, Massachusetts) chosen for its wide range of digital image processing approaches. MATLAB® is a numerical computing environment that allows matrix manipulations, plotting of functions and data, as well as implementation of algorithms. MATLAB® allows wide-area assessment of land cover to be achieved quickly and provides for a variety of image-based signal processing approaches. In our method,

we designed a MATLAB® program to coregister before and after imagery in single or multiple bands, ensuring coregistered ortho-rectification pixel to pixel on the chosen scenes. In the MATLAB®, workspace elements can then undergo matrix manipulations.

Our simplest analysis uses IKONOS. NDVI $= (\rho_{\mathrm{NIR}} - \rho_{\mathrm{Red}})/(\rho_{\mathrm{NIR}} + \rho_{\mathrm{Red}})$ analogous to Landsat's NDVI. NDVI is usually applied to vegetative land cover or our normalized media-related temporal imagery method $C_{\mathrm{T}} = (\rho_{\mathrm{After}} - \rho_{\mathrm{Before}})/(\rho_{\mathrm{After}} + \rho_{\mathrm{Before}})$, where ρ is the satellite camera's DN. Media outlets do not want or require NDVI. Human rights workers usually work with aerial or ground-based visible single-band imagery. Historically, most military aerial surveillance operations used single-band image comparison. However, a better choice would be to subtract before NDVI from the after NDVI where available. NDVI has a normalized index between modular values of 0 and 1 but is not radiometrically calibrated and is one of several normalized indices used for vegetation, soil, and other common surfaces.[18] Our imagery, except where explicitly stated, is IKONOS NDVI imagery.

2.4.2 *Matrix filter approach*

Point, line, and edge feature detection depends critically on contrast in the neighborhood of visible features. We define a high-pass filter to initially locate building outline when searching massive area images otherwise reflectance saturated and to remove low-frequency spatial pattern background detail.[18,19] Appropriate filters negatively weight neighbor pixel coefficients to enhance regions, so fine detail is emphasized. Edge or boundary extraction is extremely relevant to building detection, but the human eye is less sensitive to noise in bright areas than dark areas. However, filters may sharpen bright regions more than dark ones and flag-up areas for further manual scrutiny with reduced false alarms.

We define a mask weighting a high-pass filter to the local mean. The filter approach will take a 3×3 image field window centered on Z_5: $\begin{matrix} Z_1 & Z_2 & Z_3 \\ Z_4 & Z_5 & Z_6 \\ Z_7 & Z_8 & Z_9 \end{matrix}$. For example, with an equal weighted mask, the filter is $\begin{matrix} 1 & 1 & 1 \\ 1 & 1 & 1 \\ 1 & 1 & 1 \end{matrix}$ so $Z_{\mathrm{average}} = 1/9\Sigma_{i=1}^{9} Z_i$. The central window pixel is termed the origin. For a 3×3 sample centered on a window pixel (origin) of say 100: $\begin{matrix} 0 & 50 & 0 \\ 50 & 100 & 50 \\ 0 & 50 & 0 \end{matrix}$, then

$$Z_{\mathrm{average}} = 1/9(0 + 50 + 0 + 50 + 100 + 50 + 0 + 50 + 0) = 33.$$

A weighted sharpening high-pass filter will perform a sliding neighbor operation on the origin $\begin{matrix} -1 & -1 & -1 \\ -1 & 9 & -1 \\ -1 & -1 & -1 \end{matrix}$ so that

$$\begin{aligned} Z_{\mathrm{average}} = 1/9(&-1 \times 0 - 1 \times 50 - 1 \times 0 - 1 \times 50 - 1 \times 50 + 9 \\ &\times 100 - 1 \times 50 - 1 \times 0 - 1 \times 50 - 1 \times 0) = 77.8, \end{aligned}$$

a higher resultant value for the origin pixel with the high-pass filter than without it. This simple high-pass filter may then be considered as a convolution application of spatial filtering performed on the original, unprocessed image.

3 Results and Discussion

3.1 *Satellite Imagery of Porta Farm, Taken Before and After the Land Clearance*

Figure 3(a), the before land clearance image, shows Porta Farm densely inhabited (July 25, 2000) while Fig. 3(b), the after land clearance image, shows the same area (September 15, 2006).

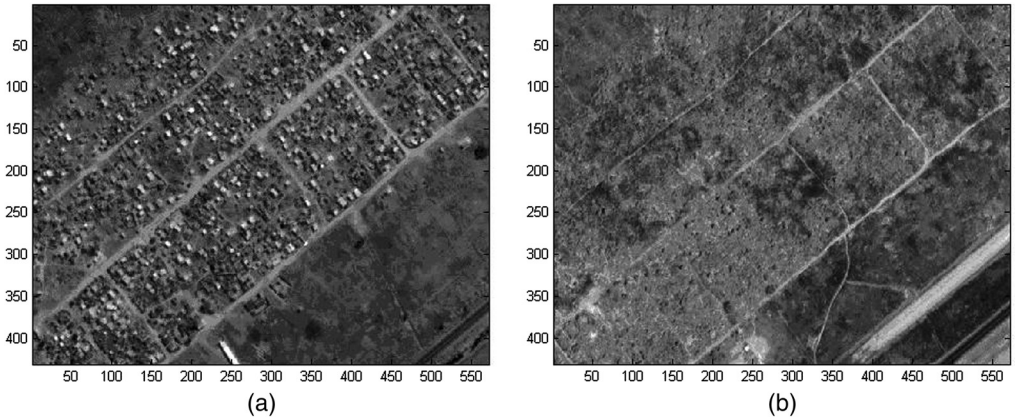

Fig. 3 (a) Before land clearance subimage plotted in colormap (gray). (b) After land clearance subimage plotted in colormap (gray).

The full extent of the man-made clearance in the imagery archive award for the second date lies slightly outside the area of the first imagery award date and is cut off from the bottom left of Fig. 3(a). Changes between the two images are dramatic; no dwellings are present in Fig. 3(b), with a few new structures added. It is unclear if these new structures are occupied, without conducting ground truthing. Removed building characterization (Fig. 4 insert) was first compiled manually.[20] Initial analysis extracted GeoTiff file regions in ArcGIS 10 as discussed in Sec. 2. The Porta Farm settlement width was 257 m, length 648 m, with 166536 m^2 total coverage.

Full Porta Farm discussion is given elsewhere,[20] but from the National Family Planning Council family size data,[21] the internally displaced people estimate for this clearance section is given, c. 6190. Individual building removal mapping was created in ArcGIS 10 (Fig. 4). United 3 Nations reports confirmed the location with a timestamp.

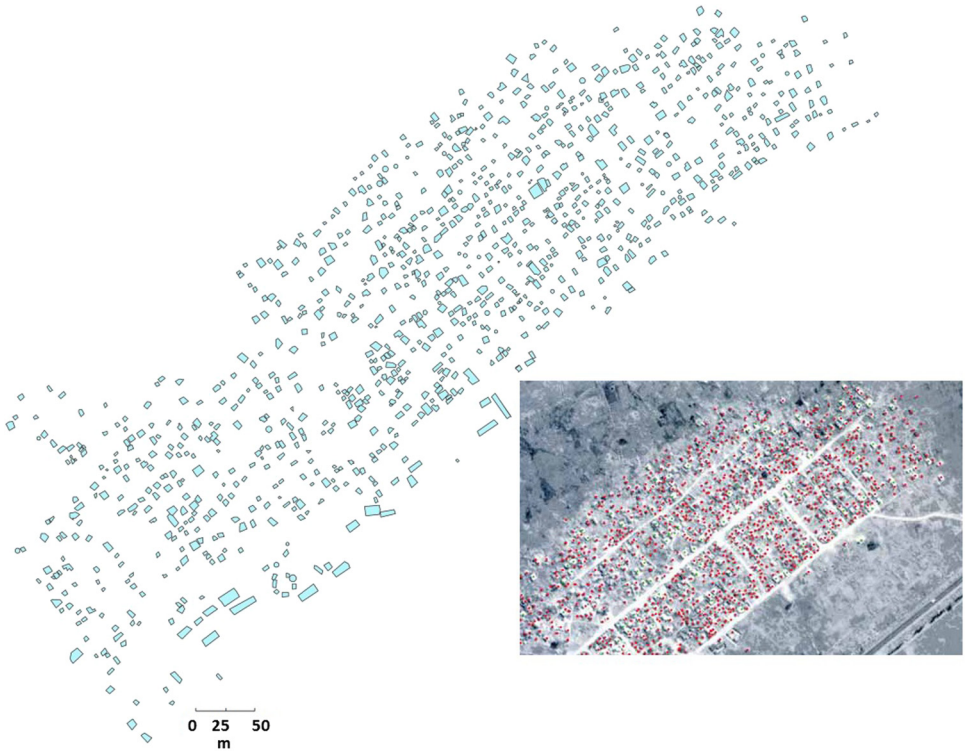

Fig. 4 Overview of Porta Farm removed buildings, plotted in ArcGIS 10. Buildings removed/destroyed. Color code: red = small dwellings, green = large buildings: possible commercial/civic/public facilities.

Previous clearance work revealed structure removal, such as hut circles, structural outlines, fire marks, etc.[6] Sometimes buildings are removed in stages, but in this case, the clearance was accomplished in just a few weeks.

3.2 *Main Inhabited Area Removal*

To identify large-scale clearance with minimal human input, a predetection nonradiometric MATLAB® process helps locate large building change areas quickly, without IKONOS radiometric calibration. Panchromatic data for both dates were examined and coregistered separately before land clearance [Fig. 3(a)] and after land clearance images [Fig. 3(b)] for building identification. Difference values fluctuate greatly, so using the normalized temporal change stated in Sec. 2.3 NDVI-like plots allows large-area normalization. Temporal change highlights residential areas surrounded by subsistence farmland (north) of varied sizes and shapes (Fig. 5).

Positive contrast is seen in some regions, e.g., road construction (southeast quadrant pixel 400, 45° southwest to northeast) with many pixel-sized noise-like dwellings on the usual search-scale. Median-based image processing may remove actual point salt-and-pepper noise yet preserve building or real artifacts with noise-like appearance. It may be possible to evaluate internally displaced people levels by measuring road occupancy after initial Baghdad assessments,[22] or with morphological operations to detect vehicle-free highways.[23] Automated road extraction with hybrid genetic algorithms or cluster analysis[24] has previously determined farm edges through segmentation,[25] but this is unnecessary in simple building change detection for human rights work.

3.3 *Section South of Porta Farm*

Nonradiometric NDVI was analyzed before [Fig. 6(a)] and after [Fig. 6(b)] for at-aperture apparent reflectance values in overlapped regions with IKONOS red and IKONOS NIR bands both coregistered in sharp definition using the NDVI workflow diagram (Fig. 2) and NDVI equation discussed in Sec. 2.4.1.

South of the clearance is mostly new horticulture or road building [Fig. 6(b)]. Most data lie in the range of 0 to 0.5 with large areas of low nonradiometric NDVI; man-made boundary and field line delineations are best viewed in this range. Nonradiometric NDVI range selection can show linear field features, change areas, chlorophyll extraction without manual manipulation,[12] and the ability to monitor the vernal advancement of natural vegetation.[26]

This work considers space-based monitoring for human rights observation and is not concerned specifically with calibration. However, an appropriate radiometric calibration (6SV) method (Fig. 2) corrected at-aperture spectral radiance to provide normalized NDVI for pixels at earth's surface for our IKONOS 2 multispectral data [Fig. 6(c)]. Normalization changes

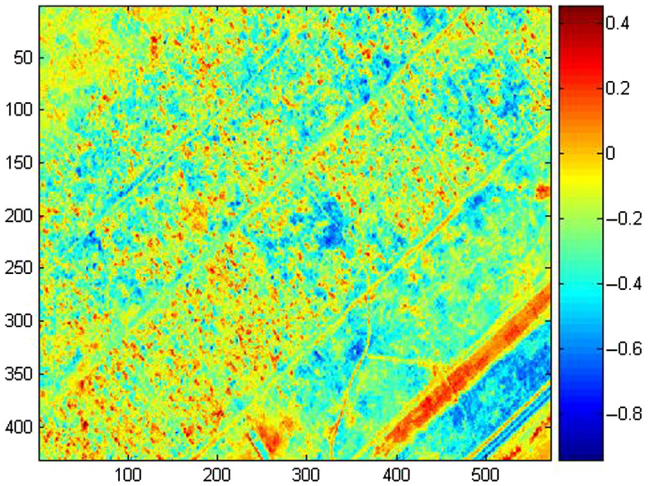

Fig. 5 Normalized media-related temporal change plotted in colormap (jet).

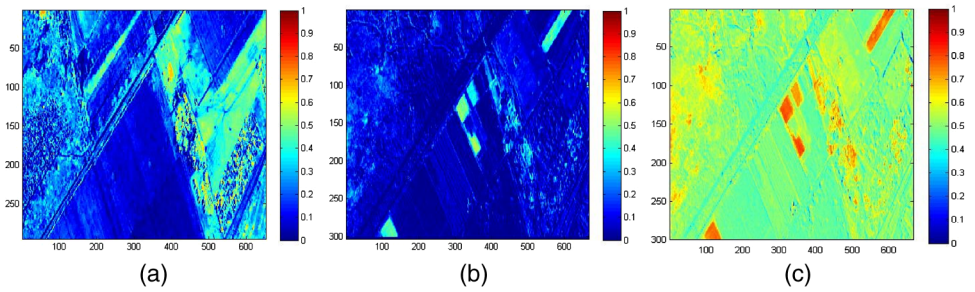

Fig. 6 (a) Before land clearance: nonradiometrically calibrated NDVI-like image, plotted in colormap (jet). (b) After land clearance: nonradiometrically calibrated NDVI-like image, plotted in colormap (jet). (c) After land clearance: radiometrically calibrated at surface NDVI image, plotted in colormap (jet).

contrast magnitude but retains features observed previously [see Figs. 6(b) and 6(c), respectively, for comparison].

Correct reflectance is vital to compare data accurately with predicted reflectance as a function of incident angle derived from a wavelength-dependent optical permittivity scattering matrix formalism.[27]

Another Zimbabwe land study identified roads beside minefields, lost minefield perimeter vegetation, or mixed agricultural area regeneration from remotely sensed data.[28] In another agricultural study, sudden reflectance change was associated with crops and revegetation associated with abandoned agricultural land on imagery separated by a minimum of 3 years,[29,30] a requirement met over our data period. Witmer and O'Loughlin[10] also examined the Bosnia–Herzegovina conflict Landsat imagery, developing vegetation detection algorithms.

3.4 *Building Outline Detection Using a High-Pass Filter*

We applied the high-pass filter defined in Sec. 2, intended for searching massive reflectance saturated imagery areas, to a test image to locate building outlines and remove low-frequency spatial pattern background.

The weighted sharpening high-pass filter used to perform a sliding neighbor operation on the origin, $\begin{matrix}-1 & -1 & -1\\ -1 & 9 & -1\\ -1 & -1 & -1\end{matrix}$, was applied to the selected image region [Fig. 7(a)].

The result of the applied high-pass filter is given in Fig. 7(b) in grayscale. Figure 7(b) shows a grayscale high-pass filter change, eliminating much of the background terrain (homogeneous light and dark regions) but still shows vegetation (negative dark areas) with most change occurring at the scale midpoint (zero level). Roofs give large $\pm$ edge changes, from high (saturated) reflectance, plunging into adjacent dark shadow. Vegetation edges are less dramatic but still have shadow. An absolute change plot for a high-pass filter was considered an acceptable way to improve edges as $\pm$ built/shadow changes combine, enhancing bright positive edges (color) with high built (straight) edges [Fig. 7(c)].

The high-pass filter does remove large bright areas (e.g., the southwest quadrant below the long white buildings) while retaining defined built edges. High reflectance regions next to low reflectance regions now produce a greater uniform area of isotropic field across the images, e.g., near (275, 50).

Varied range limits (the saturation threshold) can discriminate sharp defined edges (e.g., buildings) and to a lesser extent vegetation and tracks (more jagged edges). Future work will use a median rank-order filter to analyze the window and remove noise, as well as a variety of other image-based filters. No suitable comparison currently in the literature has discussed the effectiveness of our high-pass filter spatial filtering approach against other techniques for man-made land clearances or similar humanitarian applications using high-resolution satellite imagery.

However, it is clear that one alternative to feature manipulations we have implemented in the spatial domain could consider image analysis of the frequency domain. With a frequency-domain

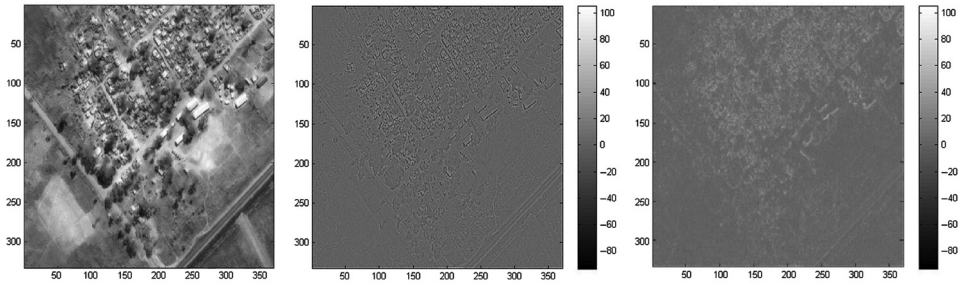

Fig. 7 (a) Original red visible band grayscale imagery showing buildings plotted in colormap (gray). (b) Filtered results for red visible band grayscale imagery plotted in colormap (gray). (c) Absolute value of filtered results for red visible band grayscale imagery plotted in colormap (gray).

approach, an image may be separated into its spatial frequency components through application of a suitable Fourier transform mathematical operation. A recent comparative study of image enhancement techniques related to general image fusion[31] proposed performance evaluation metrics for spatial and frequency methods, including error analysis, but performed no comparative evaluation on imagery.

4 Conclusion

Comparison of before and after IKONOS satellite imagery can provide evidence to corroborate altered land use: building removal, addition, and agricultural changes. Manual assessment was used to map Porta Farm but was time-consuming. MATLAB® software-based large-area assessment with suitable algorithms is shown to provide rapid change assessment, with false color contrast delineating man-made boundaries, e.g., fields, from natural ones, such as lake edges. A high-pass filter can also better define built edges in high reflectance imagery. Suitable MATLAB® spectral and temporal comparisons can provide radiometrically calibrated and non-radiometrically calibrated NDVI products to quantify and visualize a wide range of human rights-related issues. The use of automation and a range of digital filters in conjunction with space-based wide-scale monitoring will be of future benefit to remotely located international human rights observers.

Acknowledgments

Dr. Lavers thanks the DigitalGlobe Foundation[32] for IKONOS 2 imagery provided from the GeoEye Foundation imagery archive for this work. At the time of the award, dated March 24, 2009, this was the GeoEye Foundation. The authors also thank Mrs. Suzanne Trimel (formerly, Amnesty USA) for access to additional Porta Farm-based imagery.

References

1. N. Mabey, "Delivering climate security international security responses to a climate changed world," Whitehall Paper 69, Royal United Services Institute (2008).
2. "Zimbabwe shattered lives—the case of Porta Farm," Amnesty International and Zimbabwe Lawyers for Human Rights, Summary: 31/03/2006 AI Index: AFR 46/004/2006 (2006).
3. International Covenant on Economic, Social and Cultural Rights (ICESCR), Article 11(1) 4 (1976), http://www.ohchr.org/EN/ProfessionalInterest/Pages/CESCR.aspx (21 March 2017).
4. UNCHR, *UN Commission on Human Rights Resolution 1993/77*, Para 1 (1993).
5. C. Fegue, "Informal settlements' planning theories and policy-making in sub-Saharan Africa—from 'site' to 'people': a critical evaluation of operations 'Murambatsvina' and 'Garikai' in Zimbabwe," *Int. J. Sustainable Dev. Plann.* **2**(4), 445–460 (2007).

6. C. Lavers et al., "Application of satellite imagery to monitoring human rights abuse of vulnerable communities, with minimal risk to relief staff," *J. Phys. Conf. Ser.* **178**, 012039 (2009).
7. C. Lavers and T. Mason, "Rapid NDVI assessment in land clearance studies using high resolution satellite imagery," in *Proc. of the Remote Sensing and Photogrammetry Society Annual Conf.* (2011).
8. B. Willum, "Human rights abuses monitored with satellite imagery: myth or reality?" Master of Arts in War Studies, Kings College London (1999).
9. E. Norton, A. Ford, and P. Cheetham, "The prospection of mass graves: a multi-platform approach," in *Proc. of the Remote Sensing and Photogrammetry Society Annual Conf.* (2013).
10. D. W. Witmer and J. O'Loughlin, "Satellite data methods and application in the evaluation of war outcomes: abandoned agricultural land in Bosnia–Herzegovina after the 1992–1995 conflict," *Ann. Assoc. Am. Geogr.* **99**(5), 1033–1044 (2009).
11. American Association for the Advancement of Science, https://www.aaas.org/program/geospatial-technologies-project (21 March 2017).
12. N. E. Podger, W. B. Colwell, and M. H. Taylor, "GeoEye-1 radiance at aperture and planetary reflectance," (2011), https://apollomapping.com/wp-content/user_uploads/2011/09/GeoEye1_Radiance_at_Aperture.pdf (21 March 2017).
13. "6SV routine," http://6s.ltdri.org/ (21 March 2017).
14. S. Y. Kotchenova et al., "Validation of a vector version of the 6S radiative transfer code for atmospheric correction of satellite data. Part I: path radiance," *Appl. Opt.* **45**(26), 6762–6774 (2006).
15. R. B. Myneni et al., "The interpretation of spectral vegetation indices," *IEEE Trans. Geosci. Remote Sens.* **33**(2), 481–486 (1995).
16. "Landsat calibration," http://landsat.usgs.gov/science_calibration.php (21 March 2017).
17. K. Soudani et al., "Comparative analysis of IKONOS, SPOT and ETM+ data for leaf area index estimation in temperate coniferous and deciduous forest stands," *Remote Sens. Environ.* **102**(1–2), 161–175 (2006).
18. P. Mather and M. Koch, "*Computer Processing of Remotely-Sensed Images: An Introduction*, 4th ed., p. 155, Wiley-Blackwell, Chichester (2011).
19. T. M. Lillesand, R. W. Kiefer, and J. W. Chipman, *Remote Sensing and Image Interpretation*, 6th ed., p. 511, John Wiley & Sons, Inc., Hoboken (2008).
20. C. Lavers, "Zimbabwe—a satellite imaging analysis of the forced demolition of Porta Farm," GeoEye Foundation Report (2011).
21. Zimbabwe Census 2012 National Report, www.zimstat.co.zw/dmdocuments/Census/CensusResults2012/National_Report.pdf (14 August 2014).
22. S. Kuthadi, "Detection of objects from high-resolution images," MSc Thesis, p. 39, University of Minnesota (2005).
23. S. Kuthadi, "Detection of objects from high-resolution images," MSc Thesis, p. 35, University of Minnesota (2005).
24. H. Liu, J. Li, and M. A. Chapman, "Automated road extraction from satellite imagery using hybrid genetic algorithms and cluster analysis," *J. Environ. Inf.* **1**(2), 40–47 (2003).
25. U. Babawuro and Z. Beiji, "Satellite imagery cadastral features extractions using image processing algorithms: a viable option for cadastral science," *Int. J. Comput. Sci.* **9**(4), 30–38 (2012).
26. J. W. Rouse, Jr. et al., "Monitoring the vernal advancement and retrogradation (green wave effect) of natural vegetation," Progress Report RSC 1978-1, p. 93, Texas A&M University, College Station (1973).
27. D. Ko and J. R. Sambles, "Scattering method for propagation of radiation in stratified media: attenuated total reflection studies of liquid crystals," *J. Opt. Soc. Am. A* **A5**, 1863–1866 (1988).
28. B. H. P. Maathuis, "Remote sensing based detection of minefields," *Geocarto Int.* **18**(1), 51–60 (2003).
29. M. E. Bauer, "Spectral inputs to crop identification and condition assessment," *Proc. IEEE* **73**(6), 1071–1085 (1985).

30. P. Coppin et al., "Digital change detection methods in ecosystem monitoring: a review," *Int. J. Remote Sens.* **25**(9), 1565–1596 (2004).
31. S. Khidse and M. Nagori, "A comparative study of image enhancement techniques," *Int. J. Comput. Appl.* **81**(15), 28–32 (2013).
32. Digital Globe Foundation (2017), www.digitalglobefoundation.org/ (21 March 2017).

Chris R. Lavers is an engineering physicist, specializing in remote sensing and maritime electromagnetic sensing issues, and has taught maritime and remote sensing modules at the University of Plymouth at Britannia Royal Naval College (BRNC) since 1993. He has published numerous papers and articles, and five books in the REEDS Marine Engineering and Technology Series. He is a subject-matter expert (radar and telecommunications) at BRNC, Dartmouth, United Kingdom.

Travis Mason is an oceanographer, specializing in coastal hydrodynamics and sediment transport. She is the director of the Channel Coastal Observatory, which is the data management center for the National Network of Regional Coastal Monitoring Programmes of England. She is particularly involved with the programmes' extensive coastal wave and tide network and also took the lead for the introduction of order 1a bathymetry of the nearshore region.

Queries

1. Please check whether the edits made to the sentence "Our simplest analysis uses..." retained the intended meaning.

2. Please note that inline matrices are treated as display equation as per style. Please check.

3. Please clarify the usage "c. 6190."

4. As per style, internet references should follow the following style. Author(s), "Title of document," Title of complete work (if relevant), date of publication or last revision. Kindly check for References 3, 11, 13, 16, 21, and 32.

5. This query was generated by an automatic reference checking system. The DOI for Reference 25 could not be located in the CrossRef database. While this reference may be correct, we ask that you check it for accuracy so we can provide as many DOI links to the referenced article as possible.

Funding Information

The authors have identified the following funders and award numbers, either on the submission form at the time of submission or in the Acknowledgments of the manuscript. Please check this list of funding agencies and make any necessary corrections using the full and official name of the funding organization. You may also wish to edit the Acknowledgments, if needed. This information may be used to help SPIE comply with funding reporting mandates.

- DigitalGlobe Foundation; Funder ID http://dx.doi.org/10.13039/100010916